Geomechanics and Engineering, *Vol. 17, No. 1 (2019) 81-95*
DOI: https://doi.org/10.12989/gae.2019.17.1.081

Full-scale investigations into installation damage of nonwoven geotextiles

Ehsan Amjadi Sardehaei[1a], Gholamhosein Tavakoli Mehrjardi[*1] and Andrew Dawson[2b]

[1]Department of Civil Engineering, Faculty of Engineering, Kharazmi University, Tehran, Iran
[2]Nottingham Transportation Engineering Centre, University of Nottingham, Nottingham, U.K.

(Received June 13, 2017, Revised December 2, 2018, Accepted December 11, 2018)

Abstract. Due to the importance of soil reinforcement using geotextiles in geotechnical engineering, study and investigation into long-term performance, design life and survivability of geotextiles, especially due to installation damage are necessary and will affect their economy. During installation, spreading and compaction of backfill materials, geotextiles may encounter severe stresses which can be higher than they will experience in-service. This paper aims to investigate the installation damage of geotextiles, in order to obtain a good approach to the estimation of the material's strength reduction factor. A series of full-scale tests were conducted to simulate the installation process. The study includes four deliberately poorly-graded backfill materials, two kinds of subgrades with different CBR values, three nonwoven needle-punched geotextiles of classes 1, 2 and 3 (according to AASHTO M288-08) and two different relative densities for the backfill materials. Also, to determine how well or how poorly the geotextiles tolerated the imposed construction stresses, grab tensile tests and visual inspections were carried out on geotextile specimens (before and after installation). Visual inspections of the geotextiles revealed sedimentation of fine-grained particles in all specimens and local stretching of geotextiles by larger soil particles which exerted some damage. A regression model is proposed to reliably predict the installation damage reduction factor. The results, obtained by grab tensile tests and via the proposed models, indicated that the strength reduction factor due to installation damage was reduced as the median grain size and relative density of the backfill decreases, stress transferred to the geotextiles' level decreases and as the as-received grab tensile strength of geotextile and the subgrades' CBR value increase.

Keywords: geotextiles; installation damage; grab tensile strength; retained tensile strength; strength reduction factor

1. Introduction

The advent of oil industries and polymer sciences resulted in the development of geotextiles to solve some technical problems in civil engineering. They have been extensively applied in soil reinforcement of geotechnical projects such as embankments over soft subgrades, road construction, slopes, retaining walls and buried pipelines (Wang *et al.* 2011, Tavakoli Mehrjardi *et al.* 2013, Naeini and Gholampoor 2014, Portelinha *et al.* 2013 and 2014, Tandel *et al.* 2014, Deb and Konai, 2014, Hosseinpour *et al.* 2015, Viera *et al.* 2015, Kim *et al.* 2015, Costa *et al.* 2016). Geotextiles can potentially lose some of their original tensile strength due to various destructive impacts such as the stresses exerted during installation, due to creep and from environmental conditions. For instance, Vieira and Pereira (2015) studied the chemical and environmental degradation induced by a recycled construction and demolition waste on the short-term tensile behavior of two geosynthetics (a uniaxial HDPE geogrid and a nonwoven PP geotextile reinforced with PET yarns). As expected the degradation induced by the recycled construction and demolition waste after 6 months of exposure was not very expressive. The primary reduction factor applied to the tensile strength of the geotextiles is due to installation damage. In fact, during the installation process, geotextiles may encounter more stresses than during their service life, with the appearance of cuts, frays and general abrasion. Koerner and Koerner (1990) exhumed 75 different geotextiles and geogrids from 48 construction sites and assessed the retained tensile strength after installation and excavation. The results revealed that coarse, irregular and frozen subgrades, poorly graded cover soil with large particles, small lift thicknesses and heavy construction equipment created severe damage. Furthermore, Allen and Bathurst (1994) summarized the results of tensile load-strain tests performed on different geosynthetic reinforcement products in site-damaged and undamaged conditions. They observed greater loss of modulus for nonwoven geotextiles compared with woven geotextiles and geogrids, owing to the thinner fibers employed by nonwoven geotextiles. Greenwood and Brady (1992) and Richardson (1998) showed that the reduction factor due to installation damage and the frequency of damage increased when increasing the backfill grain size and number of passes.

Bathurst *et al.* (2011) analyzed a database of results from field installation damage trials on 103 different geosynthetic products. This database had been collected from 20 different sources for Load and Resistance Factor Design (LRFD) calibration of reinforced soil structures. In this study, the formulation of the limit state for reinforcement tensile rupture is developed and the

∗Corresponding author, Assistant Professor
E-mail: ghtavakoli@khu.ac.ir
[a]Postgraduate
[b]Associate Professor

http://www.techno-press.org/?journal=gae&subpage=7 ISSN: 2005-307X (Print), 2092-6219 (Online)

component strength-reduction bias statistics identified. Installation damage bias statistics were reported for six different categories of geosynthetic and four categories of backfill soils classified according to the D_{50} particle size. They showed how bias statistics together with load and resistance factors for the geosynthetic rupture limit state function can be used to calculate the probability of failure using Monte Carlo simulation and demonstrated the sensitivity of probability of failure to the magnitude of the installation damage bias statistics.

Most researchers emphasize that the level of damage depends directly on the weight, type and number of passes of the compaction equipment. On the other hand, compaction of the backfill by a lighter compactor tends to reduce the installation damage of the geotextiles (Watts and Brady 1994, Watn *et al.* 1998, Elvidge and Rymond 1999, Pinho-Lopes and Lopes 2013, Hufenus *et al.* 2005). Hufenus *et al.* (2005) found out that the survivability of geosynthetics (specifically geogrids and geotextiles) primarily depends on the type of geosynthetic (fabric design, type of tensile element) and, secondarily, on the nature of the polymer. The installation damage of individual geotextiles is predominantly influenced by the size distribution and geometry of the soil particles as well as the compaction energy. Nikbakht and Diederich (2008) used the area under the stress-strain curve in wide-width tensile tests as an indication of the energy absorption abilities of geotextiles. They showed that the retained strength increased and strength reduction factor decreased with increasing ability to absorb energy.

AASHTO M288-08 categorizes three different classes for geotextiles (1, 2 and 3) based on their survivability, according to the geotextiles' application and their physical and mechanical properties. Class 1 is specified for more severe or harsh installation conditions where there is a greater potential for geotextile damage while Classes 2 and 3 are specified for less severe conditions (Watn *et al.* 1998, Richardson 1998, Elvidge and Rymond 1999, Nikbakht and Diederich 2008, Rosete *et al.* 2013, Pinho-Lopes and Lopes 2013, Carlos *et al.* 2015). Richardson (1998) clarified that installation damage to geotextiles can be minimized by applying at least 15cm initial lift of fill over the geotextiles prior to compaction and a maximum stone size in the initial lift to less than ¼ of the lift thickness. In such a situation, a minimum survivability "Class 2" geotextile would be needed (although Class 1 is preferable).

FHWA-NHI-00-044 presented installation damage reduction factors for different types of geotextiles, depending on the backfill soil grading. This guideline states that, in the absence of project specific data, the largest indicated reduction factors should be used. Although, there have been many studies into the installation damage of geotextiles, yet there is a lack of investigation into the response of geotextiles after installation with respect to a suite of different parameters such as aggregate size, subgrade stiffness, relative density of the backfill and class of geotextile. Therefore, the specific aims of this study are:

- To investigate geotextile damage by use of a series of full-scale field tests,
- To investigate and to compare effects of the above-mentioned parameters on the installation damage reduction factor of geotextiles,
- To formulate the relation between reduction factors owing to installation damage and the afore-mentioned parameters,
- To correlate the installation damage reduction factor of geotextiles to these factors,
- To gain understanding of the caused damage by visual inspection of the geotextiles, before and after installation.

The study has been performed on full-scale field installations and should give responses that are broadly similar to those that which would be expected in normal practice.

2. Test materials

2.1 Backfill materials

In contrast with most experimental studies which investigate combinations of geotextiles and well-graded soils, this study, in order to have better accuracy and assessment of the effect of particle size, used poorly-graded backfill. These kinds of backfill are more common when a geotextile's reinforcement application involves ballast or

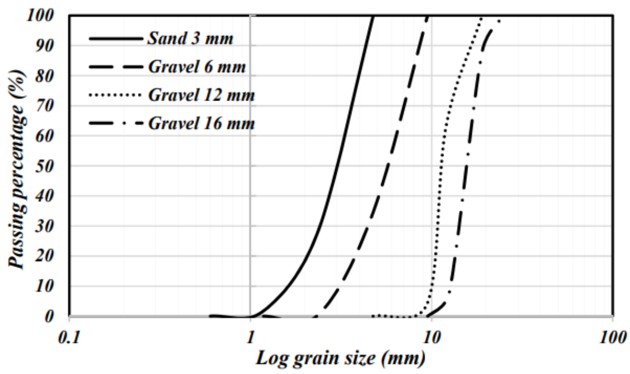

Fig. 1 Grain size distribution curves for backfill materials

Table 1 Physical properties of backfill materials

Description	Sand 3 mm	Gravel 6 mm	Gravel 12 mm	Gravel 16 mm
Coefficient of uniformity, Cu	2.125	2.14	1.33	1.27
Coefficient of curvature, Cc	1.19	1.08	0.95	0.96
Effective grain size, D_{10} (mm)	1.52	2.92	9.75	13.6
D_{30} (mm)	2.42	4.43	11	15
Median grain size, D_{50} (mm)	3.1	5.9	12.5	16.5
D_{60} (mm)	3.23	6.24	13	17.3
Specific gravity, Gs	2.419	2.494	2.546	2.604
Moisture content (%)	Dry	Dry	Dry	Dry
Percentage of fractured particles* (%)	85	80	83	82
Classification (USCS)	SP	GP	GP	GP

*The percentage of soil grains by weight in which the particles are not completely spherical and round. This was determined according to the ASTM D 5821-13

Table 2 Physical properties of subgrades

Description	CS	FS
Coefficient of uniformity, Cu	10.95	7.16
Coefficient of curvature, Cc	2.86	1.55
Effective grain size, D_{10} (mm)	0.42	0.183
D_{30} (mm)	2.35	0.61
Median grain size, D_{50} (mm)	3.65	1.00
D_{60} (mm)	4.6	1.31
CBR soaked (%)	49	27
Moisture content (%)	5	5
Maximum dry unit weight, $\gamma_{d\,(max)}$ (kN/m^2)	19.36	17.18
Classification (USCS)	SW	SW

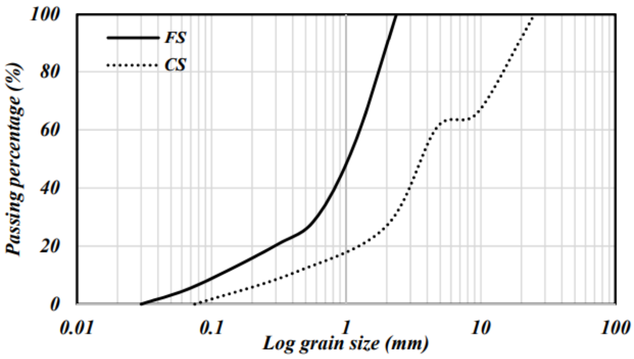

Fig. 2 Grain size distribution curves for subgrades

Table 3 Engineering properties of the geotextiles used

Description	Test methods	GT_3	GT_2	GT_1
Mass per unit area (g/m^2)	ASTM D 5261-10	292	319	508
Grab tensile strength (N)	ASTM D 4632-15a	650	800	1350
Grab elongation (%)	ASTM D 4632-15a	> 50	> 50	> 50
Trapezoidal tear strength (N)	ASTM D 4533-15	310	385	600
CBR puncture (N)	ASTM D 6241-14	900	1500	2500
Class	AASHTO M 288-08	3	2	1

backfill behind the retaining walls. Thus, four types of uniformly graded (poorly-graded) soils were used as backfill materials with the median grain size (D_{50}) of 3, 6, 12 and 16 mm. The properties of these backfill materials, which are classified as SP and GP in the unified Soil classification System, are summarized in Table 1. Also, the grading of backfill materials is graphically illustrated in Fig. 1.

2.2 Subgrades

Two types of well-graded course materials namely "fine-grained subgrade, FS" and "coarse-grained subgrade, CS" were used to simulate the subgrade. The properties of these soils are presented in Table 2. In this study, "FS" and "CS" are intended to provide soft and stiff bases for geotextiles, respectively. The grading of the subgrades is presented graphically in Fig. 2.

2.3 Geotextiles

Three types of needle-punched nonwoven geotextiles, made of polypropylene, are used, representing Classes 1, 2 and 3 in accordance with AASHTO M 288-08. The engineering properties of the geotextiles are provided in Table 3 (ASTM D 4533-15, D 4632-15a, D 5261-14, D 6241-10).

3. Testing methods

3.1 Full-scale field model tests

In order to simulate the installation process of geotextiles in unpaved roads, a physical model was developed by the authors. Fig. 3 shows the schematic representation of the test setup. The test area was divided by the two kinds of subgrades ("FS":soft and "CS":stiff). Prior to the subgrades' construction, all obstacles such as trees root, grass, meadow mat and vegetative soil cover were removed. The subgrades were constructed and compacted with plane surfaces using a walk-behind tandem vibratory roller in a layer of 150mm-lift thickness, having 5% water content to achieve a relative density of at least 95%. As can be seen in Fig. 3(a), six tests can be set up in each round of installations. The test zones were surrounded by concrete frame supported by buttresses, having thickness and depth of 150 mm, to prevent spreading of the backfill during the compaction process (Fig. 3 (b)). In all installations the subgrades were next covered by geotextiles (of Classes 1, 2 or 3), each being 1000 mm × 1200 mm in plan. Then, one of the backfill materials was placed into the frame above the geotextiles over the full length of the test area (see Fig. 4). The backfill was placed in two layers, each of 50mm-lift thickness. In order to compact the backfill, the same walk-behind tandem roller was used, but this time without vibration, to achieve the desired relative density (D_r≈70%=C1 (medium dense) and D_r≈90%=C2 (very dense), using 8 and 10 roller passes, respectively) of the soils. Details of the compactor specifications are presented in Table 4. To have a better assessment of the backfill and subgrade compaction, in some installations and after backfill placement, soil densities were measured according to ASTM D1556-07. At the end of the compaction process, the backfill was carefully removed to ensure that the geotextiles could be exhumed without any additional damage. Then, visual inspections and grab tensile tests, as described in the following sections (3.2 and 3.3), were performed on the exhumed samples of geotextiles (Tavakoli Mehrjardi and Amjadi 2017).

3.2 Visual inspection

In order to inspect the installation damage caused to the geotextiles, all of the samples were first inspected by eye. To have a better visual assessment, samples of geotextiles both before and after installation, were scanned and some image processing was performed to estimate degradation in

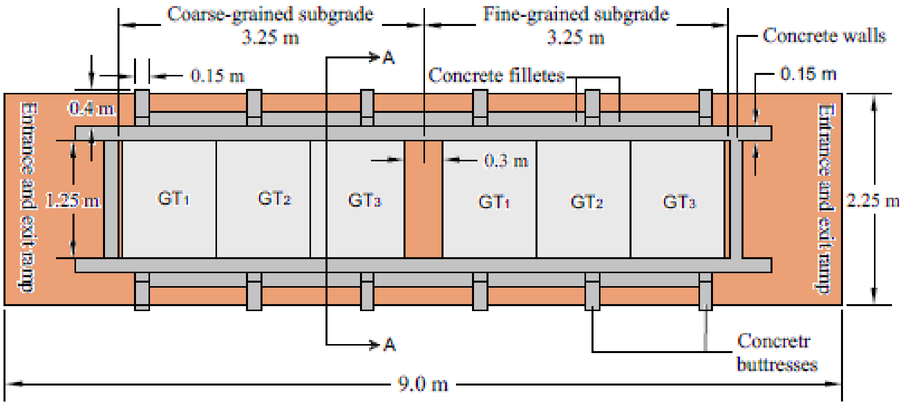

(a)

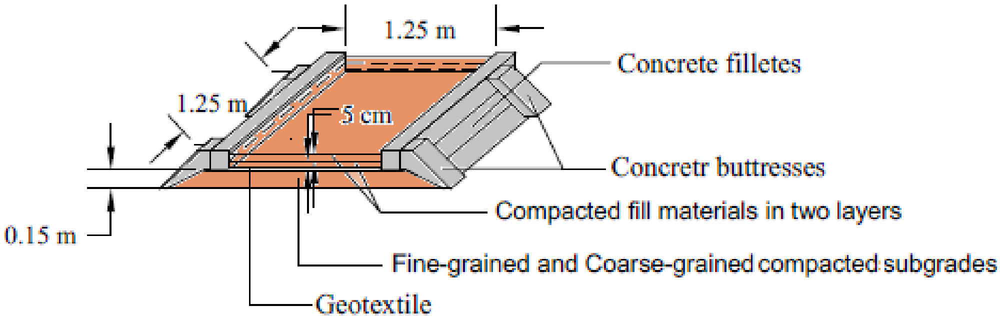

(b)

Fig. 3 Schematic representation of the test setup (a) plan (b) section A-A

(a)

(b)

Fig. 4 Photos of full-scale field tests (a) geotextile installation (b) backfill compaction

Table 4 The detail of walk-behind tandem vibratory roller

Total width (mm)	Diameter/Width of wheels (mm)	Total mass (kg)	Mass/unit area (kg/cm^2)	Speed of forward and reverse (km/h)
895	480/750	950	1.27	0-1.6

the texture of the geotextiles. The observations are reported in Section 5.1.

3.3 Grab tensile strength test

AASHTO M288-08 classifies geotextile as 1, 2 or 3 based on strength property. The grab tensile strength (ASTM D 4632-15) is used to assess the geotextile's mechanical strength under direct tension. In order to quantify the damage severity of the geotextiles, following installation, grab tensile strengths of the exhumed geotextiles were assessed and compared to the strengths obtained from specimens which had never been installed beneath the backfill. Specimens of geotextiles with dimensions of 203.2 mm × 101.6 mm were punched from the parent material. Sampling was performed according to ASTM D5818-00. Then, having placed the specimens in the test machine with a free distance of 75 mm between the clamps, the tensile testing machine applied tensile loading at a rate of 300 mm/minute till rupture takes place. During the test, grab tensile forces are accompanied by corresponding elongations which are, simultaneously, recorded. The grab tensile test was carried out on three specimens in each case and the representative mean result has been reported as retained grab tensile strength in Tables 3 and 7. The number of tests on damaged and undamaged samples (3 each) did not comply with North American practice for product certification. The WSDOT T925 (2005) installation damage test protocol calls for a minimum of five undamaged specimens and nine or more damaged specimens depending on the COV of strength values for the exhumed (damaged) specimens (Bathurst *et al.* 2011).

4. Test programme

Table 5 gives details of the test series performed in this study. For easy recognition, a system of test coding was defined (Table 6). Each test is coded in the form A-B-C-D, where "A" signifies the class of geotextile, "B" the subgrade type, "C" the backfill material and "D" the relative density of the backfill. For example, the test with the code GT1-CS-6-C1, has a geotextile of Class 1 installed on coarse-grained subgrade covered by backfill with D_{50}=6 mm and compacted with D_r=70%.

Table 5 Testing programme

Geotextiles' Class	Subgrades' CBR (%)	Relative Density (%)	Median Grain Size (mm)	No. of Tests
1	27 and 49	70 and 90	3, 6, 12 and 16	16
2	27 and 49	70 and 90	3, 6, 12 and 16	16
3	27 and 49	70 and 90	3, 6, 12 and 16	16

Table 6 Symbol of variable parameters for coding the geotextile specimens

Geotextile type	Symbol	Subgrade type	Symbol
Class 1	GT_1	Coarse-grained	CS
Class 2	GT_2	Fine-grained	FS
Class 3	GT_3		
Backfill type	Symbol	Relative density of backfill materials	Symbol
Sand 3 mm	3	70 %	C_1
Gravel 6 mm	6	90 %	C_2
Gravel 12 mm	12		
Gravel 16 mm	16		

5. Results and discussions

5.1 Visual inspection

Among the possible types of damage that can be caused by installation, the following outcomes were investigated: cutting, fraying, very fine-grained particles pushed into the texture, fiber separation, holes and local stretching of geotextiles by larger soil particles.

According to the visual inspections, there was no fraying, fiber separation nor holes. However, in all specimens, fine-grained particles with a size of about 0 to 2 mm penetrated into the texture of the geotextiles. Although, the aggregates did not puncture the geotextiles, backfills with larger particles, especially with a median grain size of 12 and 16 mm, squeezed into the texture, specifically in Class 2 and Class 3 geotextiles. An explanation may be that increasing the grain size will decrease the number of stone-stone contacts but each having a higher contact force and that, therefore, this tends to transfer more stress onto the geotextiles. As expected, geotextile Class 1, due to its greater thickness, appeared to be less damaged by the installation process than others.

5.2 Grab tensile test

As Table 7 compares the values of grab tensile strength obtained before and after installation. It might be expected that the retained tensile strength of the geotextiles (T_{ID}) should be less than the as-received tensile strength (T_0); but, as can be seen in Table 7, 14 tests out of 48 tests have retained tensile strengths more than their original strengths (for most of them, just a little larger than their original strength). This may have happened because of non-uniformity in the texture of geotextiles, resulting in strengths varying with position in the geotextiles sheet. Another cause may be due to local strain-hardening caused by fiber distortion. This matter has been observed by some previous researchers (Greenwood and Brady 1992, Allen and Bathurst 1994, Hufenus *et al.* 2005). Allen and Bathurst (1994) stated that this effect may be due to the accumulation of fine particles in the fiber matrix of geotextiles and, possibly, the result of "strain hardening" of polyolefin materials due to locked-in tensile load during compaction.

Table 7 Values of retained grab tensile strength obtained after exhumation for each test condition

Test code	Tensile strength (N)	Test code	Tensile strength (N)	Test code	Tensile strength (N)
GT_1-CS-3-C_1	1321	GT_2-FS-6-C_1	666	GT_3-CS-12-C_2	575
GT_2-CS-3-C_1	893	GT_3-FS-6-C_1	690	GT_1-FS-12-C_2	1206
GT_3-CS-3-C_1	599	GT_1-CS-6-C_2	1243	GT_2-FS-12-C_2	695
GT_1-FS-3-C_1	1397	GT_2-CS-6-C_2	662	GT_3-FS-12-C_2	704
GT_2-FS-3-C_1	743	GT_3-CS-6-C_2	605	GT_1-CS-16-C_1	1459
GT_3-FS-3-C_1	633	GT_1-FS-6-C_2	1325	GT_2-CS-16-C_1	920
GT_1-CS-3-C_2	1332	GT_2-FS-6-C_2	659	GT_3-CS-16-C_1	604
GT_2-CS-3-C_2	887	GT_3-FS-6-C_2	615	GT_1-FS-16-C_1	1222
GT_3-CS-3-C_2	676	GT_1-CS-12-C_1	1333	GT_2-FS-16-C_1	704
GT_1-FS-3-C_2	1289	GT_2-CS-12-C_1	848	GT_3-FS-16-C_1	538
GT_2-FS-3-C_2	755	GT_3-CS-12-C_1	599	GT_1-CS-16-C_2	1286
GT_3-FS-3-C_2	644	GT_1-FS-12-C_1	1387	GT_2-CS-16-C_2	597
GT_1-CS-6-C_1	1283	GT_2-FS-12-C_1	725	GT_3-CS-16-C_2	578
GT_2-CS-6-C_1	731	GT_3-FS-12-C_1	658	GT_1-FS-16-C_2	1416
GT_3-CS-6-C_1	632	GT_1-CS-12-C_2	1375	GT_2-FS-16-C_2	823
GT_1-FS-6-C_1	1237	GT_2-CS-12-C_2	750	GT_3-FS-16-C_2	634

Figs. 5 to 9 are presented to study the effects of median grain size of backfill materials, the relative density of backfill materials, the geotextiles class and the type of subgrades on the retained tensile strength of the geotextiles. In some of these figures (Figs. 5 and 6) a trend line for either all results, named "48-test", or for results where the retained tensile strengths were smaller than the as-received tensile strength, named "34-test", is illustrated. As can be seen in Figs. 5 and 6, according to the "48-test results", tensile strengths of the geotextiles have mostly decreased with increase of median grain size of the backfill. As

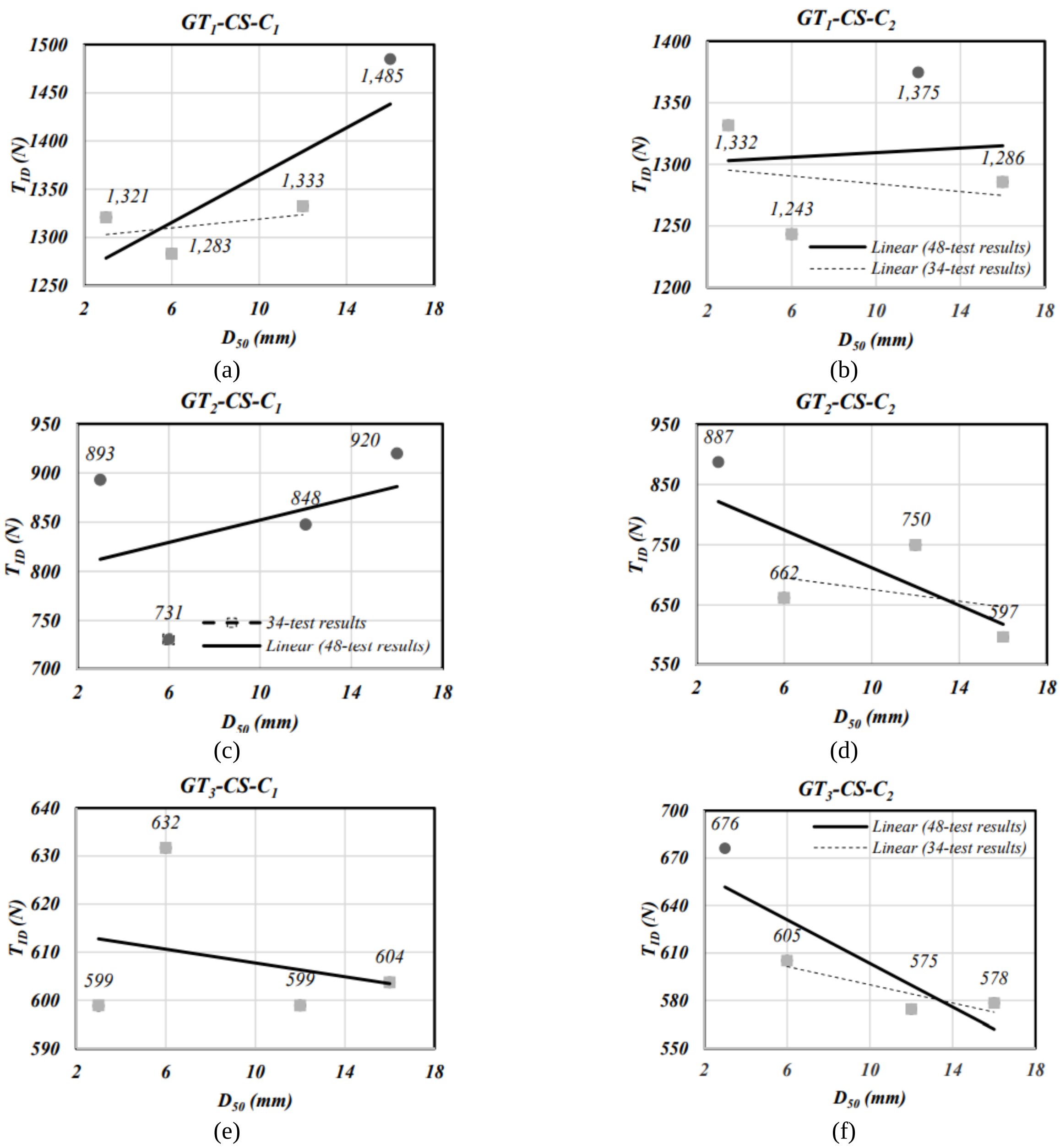

Fig. 5 Retained geotextile tensile strengths for different size backfills all on subgrade "CS". Dr=70% for (a), (c) and (e), Dr=90% for (b), (d) and (f). Solid lines and dashed lines are plotted with and without considering the "circle points", respectively. These "circle points" represent retained tensile strengths larger than the as-received tensile strengths

explained in the earlier section (5.1) on visual inspection, increasing the grain size tends to transfer more stress onto the geotextiles, leading to a reduction in the ultimate tensile strength.

From Fig. 7 shows that tensile strengths of the geotextile were mostly decreased following compaction of the backfill to the higher relative density. This is probably because the higher relative density, obtained by an increased mass of backfill over the geotextile in addition to the increased number of compactor passes, resulted in transfer of more energy on geotextile and thereby, reduction in the retained tensile strength. These results are in line with the findings of previous investigators (Greenwood and Brady 1992, Richardson 1998, Elvidge and Raymond 1999, Elias 2001, Mendes *et al.* 2007, Pinho-Lopes and Lopes 2013, Carlos *et al.* 2015).

Mechanical properties of the geotextiles are another parameter which significantly affects the installation damage. According to Fig. 8, it can be seen that by increasing the tensile strength of the geotextiles (changing the geotextiles class from 3 to 1), the survivability would be increased. As a rule-of-thumb, it is obvious that the minimum reduction factor (the ratio of as-received tensile strength to retained tensile strength of the geotextiles) equals 1.11, and belongs to geotextile Class 1 (Want *et al.* 1998, Richardson 1998, Elvidge and Raymond 1999, Nikbakht and Diederich 2008, Pinho-Lopes and Lopes 2013, Rosete *et al.* 2013, Carlos *et al.* 2015).

According to majority of the results shown in Fig. 9, the subgrade stiffness had a positive influence on the

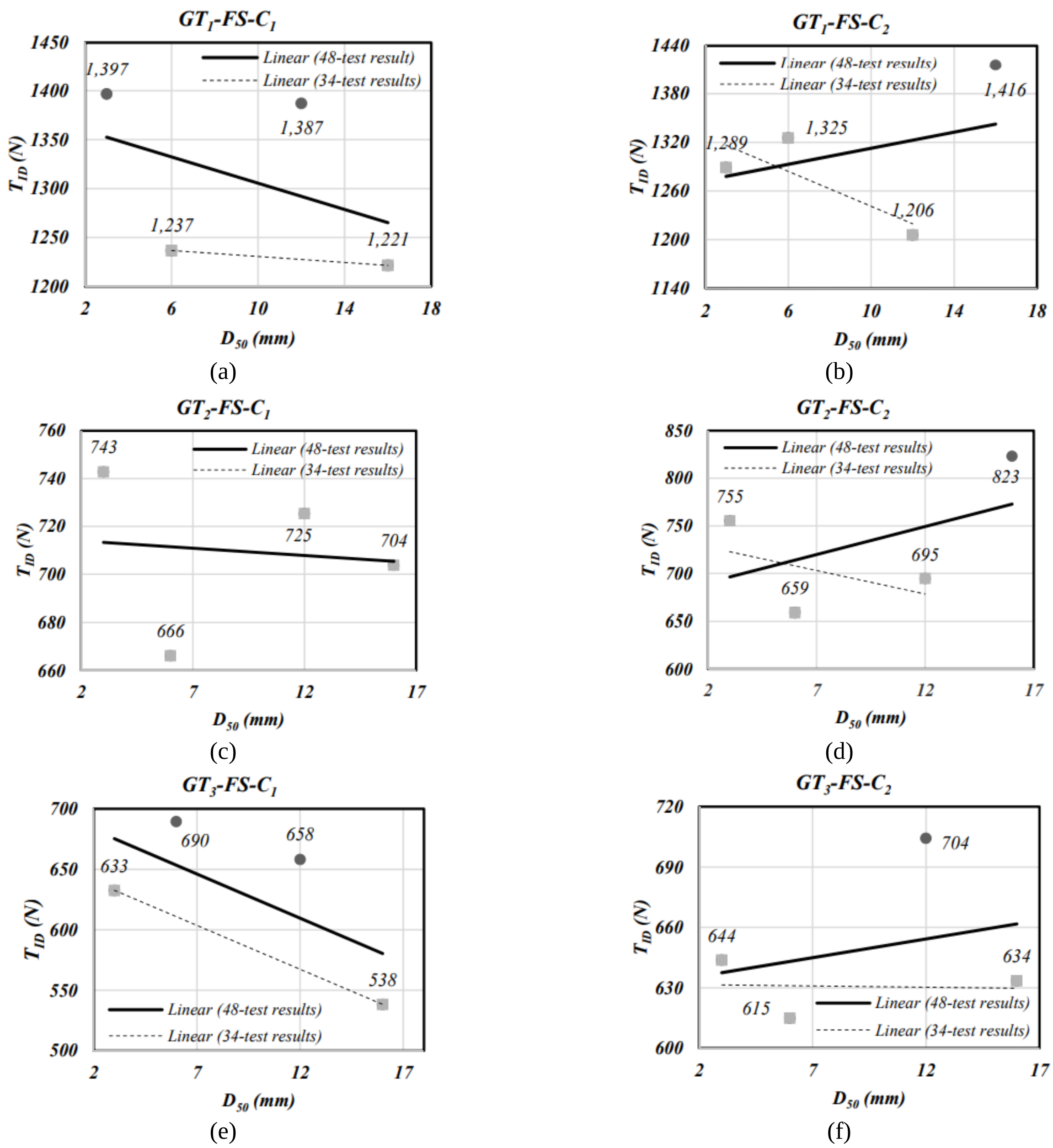

Fig. 6 Retained geotextile tensile strengths for different size backfills all on subgrade “FS”. Dr=70% for (a), (c) and (e), Dr=90% for (b), (d) and (f). Solid lines and dashed lines are plotted with and without considering the “circle points”, respectively. These “circle points” represent retained tensile strengths larger than the as-received tensile strengths

survivability of the geotextiles. It seems that reduction in the CBR value of the subgrade allowed movement beneath the geotextile, leading to more tension in the geotextile and, thereby, causing greater damage.

It should be mentioned that the impacts of relative density of the backfill and subgrade type on installation damage of the geotextiles were accompanied with some uncertainty and scatter. Perhaps, for this reason, FHWA-NHI-10-024 focuses on the grain size of backfill and geotextile type to suggest reduction factors due to installation damage.

Given that damage is widespread, even if not always discovered, the “34-test” results provide a more conservative assessment of damage. Therefore, the study continues based only on the “34-test” results.

5.3 Dimensional analysis

Dimensional analysis aims to generalize our analytical description of a problem based on background knowledge, helping with extrapolation towards the prototype case (Tavakoli Mehrjardi *et al.* 2016). Eq. (1) lists the major physical parameters influencing the retained tensile strength (T_{ID}):

• median grain size of backfill materials (D50) in meters,

• subgrade CBR expressed as a percentage,

• relative density of backfills (Dr) also expressed as a percentage,

• as-received geotextile tensile strength (T0) in Newtons, and

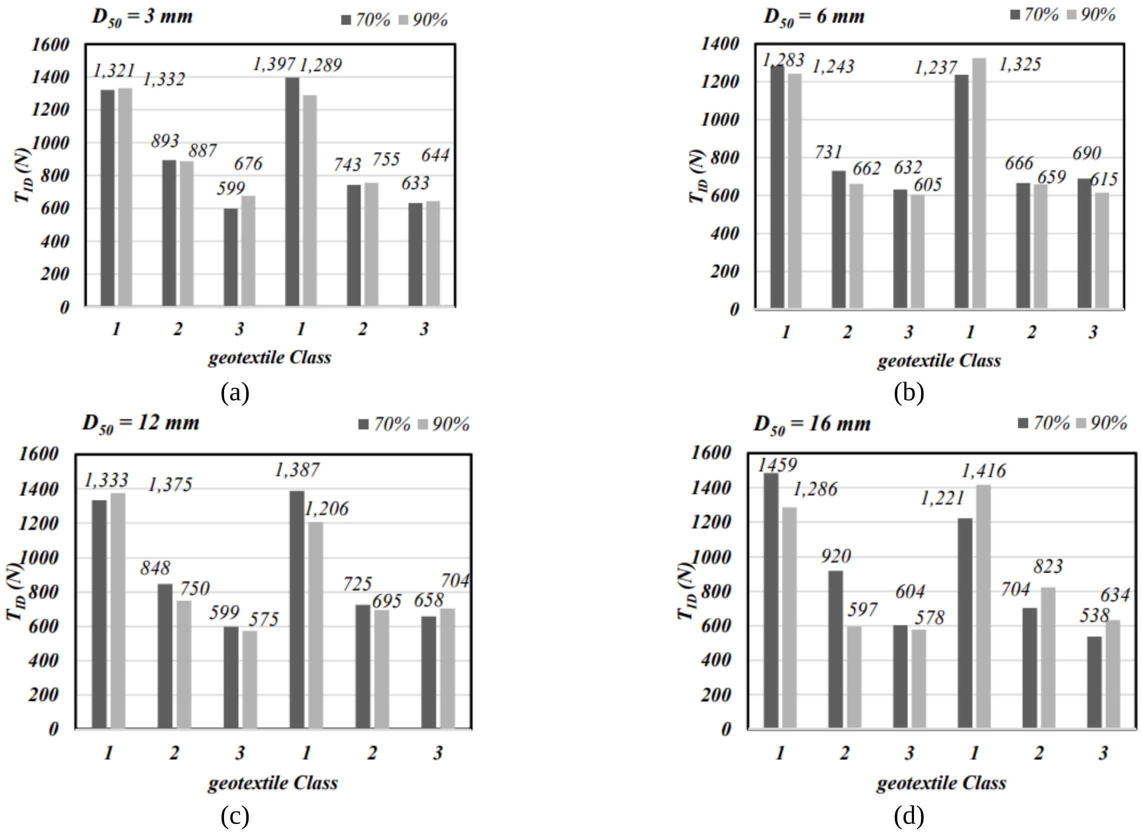

Fig. 7 Variations of retained tensile strength with respect to relative density of the backfill with (a) D_{50}=3 mm, (b) D_{50}=6 mm, (c) D_{50}=12 mm and (d) D_{50}=16 mm

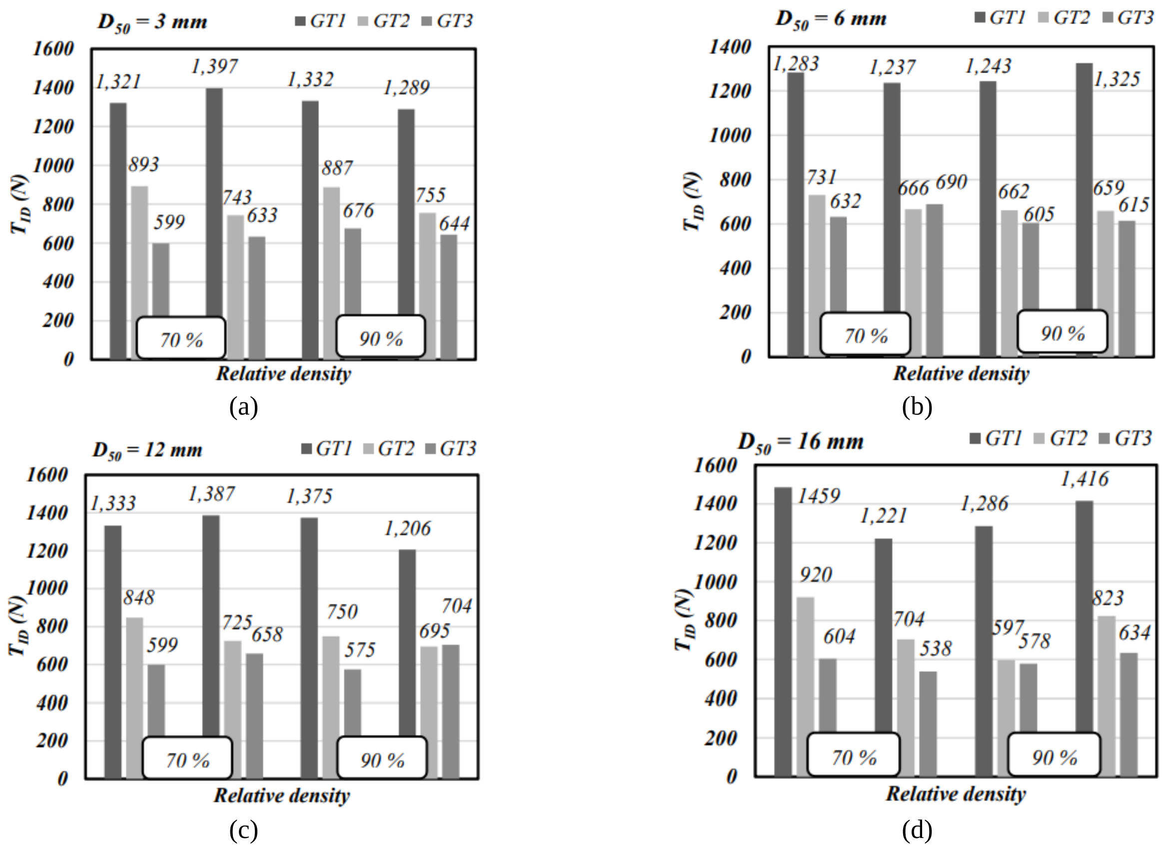

Fig. 8 Variations of retained tensile strength with respect to geotextiles' class for backfill with (a) D_{50}=3 mm, (b) D_{50}=6 mm, (c) D_{50}=12 mm and (d) D_{50}=16 mm for the two relative densities shown

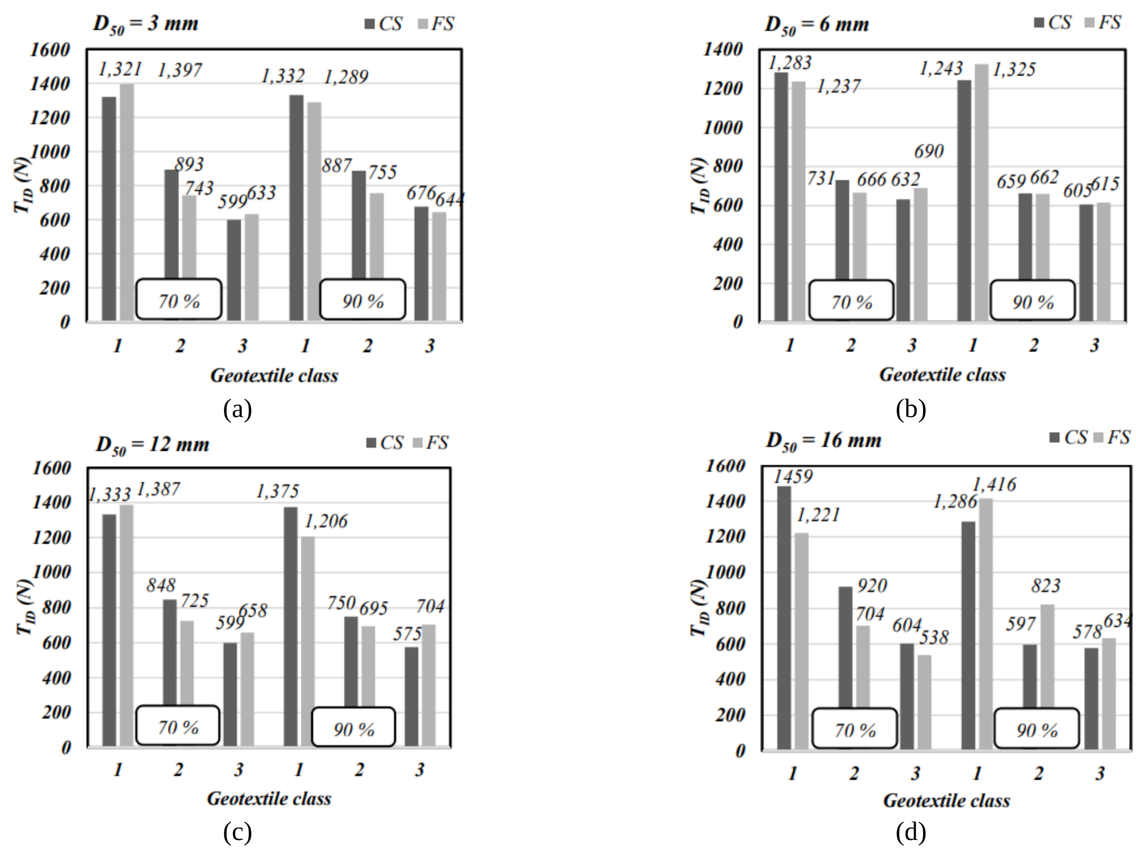

Fig. 9 Variations of retained tensile strength with respect to subgrades' CBR for backfill with (a) D_{50}=3 mm, (b) D_{50}=6 mm, (c) D_{50}=12 mm and (d) D_{50}=16 mm for the two relative densities shown

• the imposed stress over the geotextiles during installation (σ) in Pascals.

The imposed stresses on the geotextile can be estimated by considering the weight of the soil above it plus the stress propagated by the compaction energy (for instance based on the Boussinesq equation).

$$T_{ID} = f(D_{50}.CBR.D_r.T_0.\sigma) \qquad (1)$$

The equation comprises 5 parameters having two fundamental dimensions (i.e., length and force). Therefore, Eq. (1) can be reduced to 3 independent parametric groups and arranged non-dimensionally as in Eq. (2)

$$\frac{T_{ID}}{T_0} = f(\frac{T_0}{\sigma D_{50}^2}.D_r.CBR) \qquad (2)$$

Table 8 tabulates these groups for each test. The dimensionless parameter T_{ID} / T_0 is defined as the ratio of retained strength (S_r) and installation damage reduction factor (RF_{ID}) is thus the reciprocal of the value (S_r) (see Table 8). Accordingly, reduction factors due to installation of geotextiles in the backfill were obtained in the range 1~1.34. This range of values is in the line with that stated in FHWA-NHI-00-044, which suggests RD_{ID}=1.1~1.4 for nonwoven geotextiles in backfill with maximum grain size 20 mm.

Since the effects of relative density and subgrade CBR on the retained tensile strength of the geotextiles were discussed in the previous section, here the remaining parameter in Eq. (3) (T_0 / σD_{50}^2) is analyzed. As can be seen in Fig. 10, an increase of T_0 / (σD_{50}^2) tends to increase the ratio of retained strength and in turn, reduce the installation damage reduction factor. The implication of Eq. (2) is that, for a backfill with a grain size 5 times that of some reference size, then the same damage, in terms of (S_r) and (RF_{ID}), could only be expected if the as-received tensile strength of the geotextile were 25 times of that in the reference situation. With grain size of the backfill in Eq. (2) having a power of two, it is clear that damage will be much more sensitive to that than to normal stress, which has a power of only one.

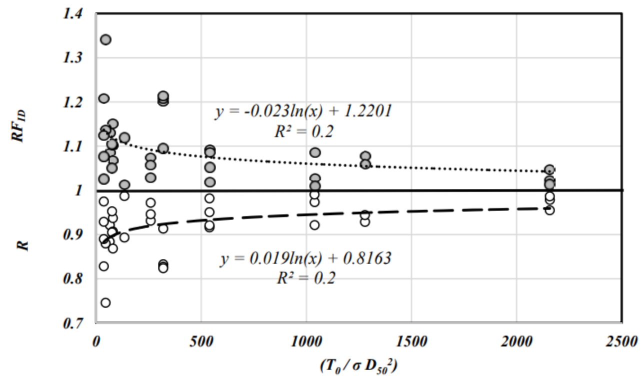

Fig. 10 Effect of the $T_0/(\sigma D_{50}^2)$ on S_r and RF_{ID}

5.4 Regression model

Multiple regression analysis attempts were made to

Table 8 Independent parameters of dimensional analysis based on test conditions

Test code	$T_0/(\sigma\ D_{50}^2)$	D_r (%)	CBR (%)	S_r	RF_{ID}
GT_1-CS-3-C_1	2158.49	70	49	0.98	1.02
GT_3-CS-3-C_1	1039.27	70	49	0.92	1.09
GT_2-FS-3-C_1	1279.11	70	27	0.93	1.08
GT_3-FS-3-C_1	1039.27	70	27	0.97	1.03
GT_1-CS-3-C_2	2157.88	90	49	0.99	1.01
GT_1-FS-3-C_2	2157.88	90	27	0.95	1.05
GT_2-FS-3-C_2	1278.75	90	27	0.94	1.06
GT_3-FS-3-C_2	1038.98	90	27	0.99	1.01
GT_1-CS-6-C_1	539.28	70	49	0.95	1.05
GT_2-CS-6-C_1	319.57	70	49	0.91	1.10
GT_3-CS-6-C_1	259.65	70	49	0.97	1.03
GT_1-FS-6-C_1	539.28	70	27	0.92	1.09
GT_2-FS-6-C_1	319.57	70	27	0.83	1.20
GT_1-CS-6-C_2	539.14	90	49	0.92	1.09
GT_2-CS-6-C_2	319.49	90	49	0.83	1.21
GT_3-CS-6-C_2	259.59	90	49	0.93	1.07
GT_1-FS-6-C_2	539.14	90	27	0.98	1.02
GT_2-FS-6-C_2	319.49	90	27	0.82	1.21
GT_3-FS-6-C_2	259.59	90	27	0.95	1.06
GT_1-CS-12-C_1	134.87	70	49	0.99	1.01
GT_3-CS-12-C_1	64.94	70	49	0.92	1.09
GT_2-FS-12-C_1	79.92	70	27	0.91	1.10
GT_2-CS-12-C_2	79.90	90	49	0.94	1.07
GT_3-CS-12-C_2	64.92	90	49	0.88	1.13
GT_1-FS-12-C_2	134.84	90	27	0.89	1.12
GT_2-FS-12-C_2	79.90	90	27	0.87	1.15
GT_3-CS-16-C_1	36.53	70	49	0.93	1.08
GT_1-FS-16-C_1	75.87	70	27	0.90	1.11
GT_2-FS-16-C_1	44.96	70	27	0.88	1.14
GT_3-FS-16-C_1	36.53	70	27	0.83	1.21
GT_1-CS-16-C_2	75.85	90	49	0.95	1.05
GT_2-CS-16-C_2	44.95	90	49	0.75	1.34
GT_3-CS-16-C_2	36.52	90	49	0.89	1.12
GT_3-FS-16-C_2	36.52	90	27	0.97	1.03

Table 9 Statistical parameters for evaluation of the proposed regression models

Estimated parameter	R^2	Standard Error (%)
Ratio of retained tensile strength	0.21	6
Installation damage reduction factor	0.2	8

quantify and enumerate Eq. (2) so that it could be used to estimate the relationships between the variable parameters. The regression model was evaluated based on coefficient of determination by minimizing the standard error. Several types of mathematical functions including cubic, quadratic, logarithmic, linear and exponential functions were considered to select an optimum regression model. Among the possibilities, the natural-logarithm function was chosen to correlate the ratio of retained tensile strength (S_r), or installation damage reduction factor (RF_{ID}), with the non-dimensional independent parameters previously identified CBR, D_r and T_0 / (σD_{50}^2). Eq. (3) and (4) show the empirical relationships that resulted.

$$R = \frac{T_{ID}}{T_0} = 0 \cdot 875 + 0 \cdot 019 \ln\left(\frac{T_0}{\sigma D_{50}^2}\right) - 0 \cdot 029 \ln(D_r) + 0 \cdot 018 \ln(CBR) \quad (3)$$

$$RF_{ID} = \frac{T_0}{T_{ID}} = 1 \cdot 09 - 0 \cdot 023 \ln\left(\frac{T_0}{\sigma D_{50}^2}\right) + 0 \cdot 046 \ln(D_r) - 0 \cdot 02 \ln(CBR) \quad (4)$$

Table 10 Comparison of the results obtained by tests and regression models

Test code	Grab tensile test		Eq. (3) and (4)		Residual value	
	S_r	RF_{ID}	S_r	RF_{ID}	S_r	RF_{ID}
GT_1-CS-3-C_1	0.98	1.02	0.97	1.03	0.01	0.01
GT_3-CS-3-C_1	0.92	1.09	0.95	1.05	0.03	0.04
GT_2-FS-3-C_1	0.93	1.08	0.95	1.05	0.02	0.02
GT_3-FS-3-C_1	0.97	1.03	0.94	1.06	0.03	0.03
GT_1-CS-3-C_2	0.99	1.01	0.96	1.04	0.03	0.03
GT_1-FS-3-C_2	0.95	1.05	0.95	1.05	0	0.01
GT_2-FS-3-C_2	0.94	1.06	0.94	1.07	0	0.01
GT_3-FS-3-C_2	0.99	1.01	0.94	1.07	0.05	0.06
GT_1-CS-6-C_1	0.95	1.05	0.94	1.06	0.01	0.01
GT_2-CS-6-C_1	0.91	1.10	0.93	1.08	0.02	0.02
GT_3-CS-6-C_1	0.97	1.03	0.93	1.08	0.04	0.05
GT_1-FS-6-C_1	0.92	1.09	0.93	1.07	0.01	0.02
GT_2-FS-6-C_1	0.83	1.20	0.92	1.09	0.09	0.11
GT_1-CS-6-C_2	0.92	1.09	0.93	1.07	0.01	0.01
GT_2-CS-6-C_2	0.83	1.21	0.92	1.09	0.10	0.12
GT_3-CS-6-C_2	0.93	1.07	0.92	1.09	0.01	0.02
GT_1-FS-6-C_2	0.98	1.02	0.92	1.09	0.06	0.07
GT_2-FS-6-C_2	0.82	1.21	0.91	1.10	0.09	0.12
GT_3-FS-6-C_2	0.95	1.06	0.91	1.10	0.04	0.05
GT_1-CS-12-C_1	0.99	1.01	0.91	1.09	0.07	0.08
GT_3-CS-12-C_1	0.92	1.09	0.90	1.11	0.02	0.03
GT_2-FS-12-C_1	0.91	1.10	0.89	1.12	0.01	0.02
GT_2-CS-12-C_2	0.94	1.07	0.90	1.12	0.04	0.05
GT_3-CS-12-C_2	0.88	1.13	0.89	1.12	0.01	0.01
GT_1-FS-12-C_2	0.89	1.12	0.90	1.12	0	0
GT_2-FS-12-C_2	0.87	1.15	0.89	1.13	0.02	0.02
GT_3-CS-16-C_1	0.93	1.08	0.89	1.12	0.04	0.05
GT_1-FS-16-C_1	0.90	1.11	0.89	1.12	0.01	0.01
GT_2-FS-16-C_1	0.88	1.14	0.88	1.13	0	0.01
GT_3-FS-16-C_1	0.83	1.21	0.88	1.14	0.05	0.07
GT_1-CS-16-C_2	0.95	1.05	0.90	1.12	0.06	0.07
GT_2-CS-16-C_2	0.75	1.34	0.89	1.13	0.14	0.21
GT_3-CS-16-C_2	0.89	1.12	0.88	1.14	0.01	0.01
GT_3-FS-16-C_2	0.97	1.03	0.87	1.15	0.10	0.12

5.4.1 Validation of the model

Table 9 shows the values of the statistical parameters for the regression models. Although the coefficient of determinations for both models were about 0.21, the standard errors of the ratio of retained strength (S_r) and of the installation damage reduction factor (RF_{ID}) were 6% and 8%, respectively. This shows that the proposed models with the probabilities of 94% and 92%, are highly representative of the measured results, even though their predictive ability is limited.

To validate the relationships expressed in Eq. (3) and (4), Table 10, containing values of the ratio of retained strength (S_r) and of installation damage reduction factor (RF_{ID}) are presented as obtained by tests results and by the empirical equations. In most of the cases, the values of the residuals (the difference between the predicted and observed values) for the ratio of retained strength (S_r) and for the installation damage reduction factor of geotextiles (RF_{ID}) were around 0.03 and 0.05, respectively. It may be noted that most of the highest residuals belong to geotextile Class 2 with more reliable modelling for Classes 1 & 3.

5.4.2 Parametric study

To study the model sensitivity and, also, the predicted values of S_r and RF_{ID}, the effect of different parameters are discussed in the following sections.

a) <u>*Effect of as-received grab tensile strength (T_0)*</u>

Fig. 11 illustrates the effect of as-received grab tensile strength of the geotextiles on the ratio of retained strength (S_r) and installation damage reduction factor of geotextiles (RF_{ID}) as estimated using Eqs. (3) and (4). The values of σ, D_{50}, D_r and CBR remain constant, equal to 100 kPa, 12 mm, 100% and 80%, respectively. According to Fig. 11, it can be found out that selection of geotextiles with higher as-received grab tensile strength results in lower installation damage.

b) <u>*Effect of transferred stress at the level of geotextile (σ)*</u>

As mentioned before, the transferred stress at the level of geotextile can be the result of the backfill's weight and of the stress propagated by the compactor energy, and having a direct role in the installation damage. Fig. 12 is presented to illustrate the effect of applied stress on geotextiles' installation damage in which T_0 =650 N, D_{50}=12 mm, D_r=70% and CBR=80%, using Eqs. (3) and (4). The results show the damage of geotextiles consequent on the transferred stress intensification. Therefore, as may have been anticipated, lighter compactors and thicker cover of the backfill materials over the geotextile should be utilized, as much as possible.

c) <u>*Effect of backfill's median grain size (D_{50})*</u>

The test results revealed that the median grain size of the backfill highly affected the retained tensile strength of the geotextiles. Fig. 13 relates the median grain size to the ratio of retained strength (S_r) and installation damage reduction factor of geotextiles (RF_{ID}). The values of T_0, σ, D_r and CBR are fixed as 650 N, 100 kPa, 70% and 80%, respectively. As can be seen, increasing the soil particle size intensifies the installation damage of the geotextiles. Therefore, using high-survivability geotextiles (i.e. class 1 per AASHTO M288-08) in backfills that contain large particle sizes is highly recommended.

d) <u>*Effect of backfill's relative density (D_r)*</u>

In order to study the impact of the backfill's relative density on the ratio of retained strength and installation damage of the geotextiles, Fig. 14 is plotted. To assess only this parameter requires that the values of T_0, D_{50}, CBR and σ remaining constant, selected here as 650 N, 12 mm, 80% and 100 kPa, respectively. According to Figs. 12 and 14, it can be concluded that the variation of installation damage reduction factor due to transferred stress and due to relative density are of the same order.

e) <u>*Effect of subgrades' CBR*</u>

Conceivably, the subgrades' CBR is effective in controlling installation damage of geotextiles due to its direct effect on the amount of extension in a geotextile layer that is under imposed stress. Fig. 15, in which T_0 =650 N, D_{50}=12 mm, D_r=70% and σ =100 kPa, shows how much the bearing capacity of the subgrades can influence the survivability of the geotextiles from installation damage. The results confirm the continued weakness of geotextiles that are placed on weaker subgrades. FHWA HI-95-038 recommends that higher survivability geotextiles should be used when the subgrade has low shear strength.

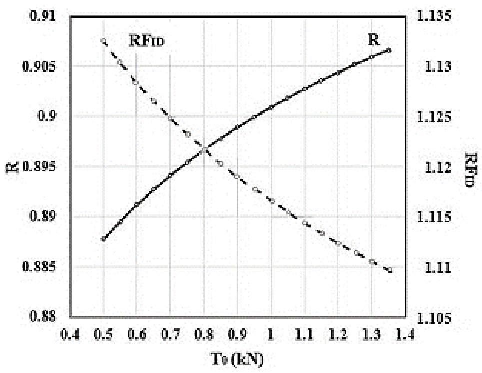

Fig. 11 Effect of as-received grab tensile strength of the geotextiles (T_0) on geotextiles' survivability

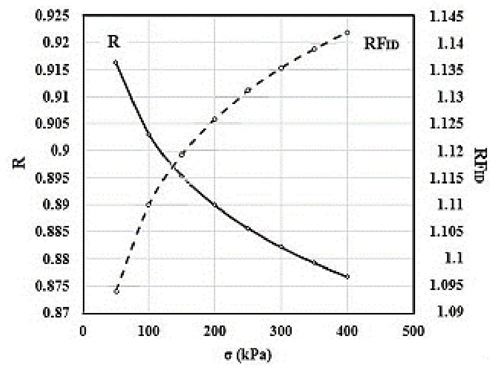

Fig. 12 Effect of transferred stress level (σ) on geotextiles' survivability

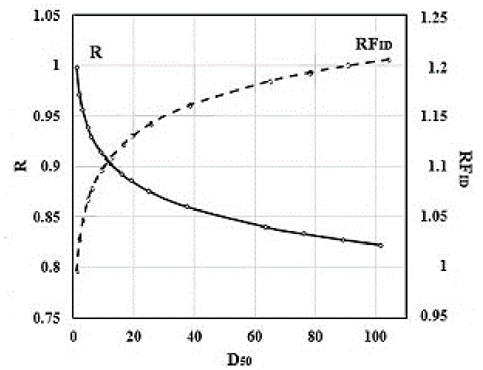

Fig. 13 Effect of backfill's median grain size (D_{50}) on geotextiles' survivability

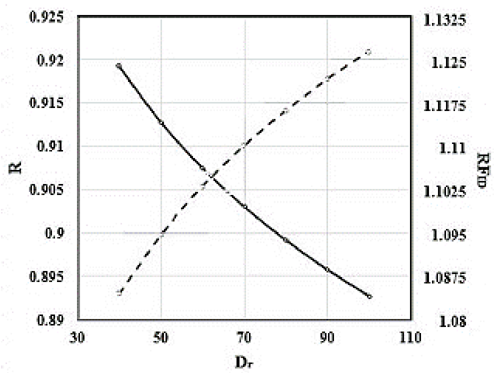

Fig. 14 Effect of backfill's relative density (D_r) on geotextiles' survivability

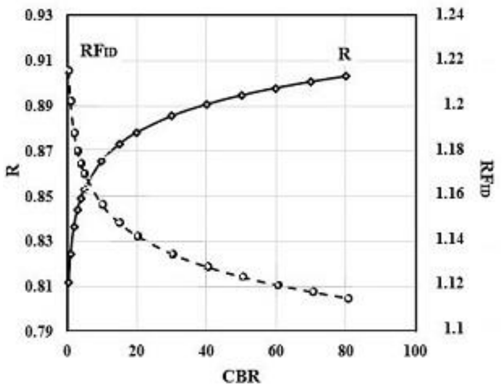

Fig. 15 Effect of subgrade' CBR on geotextiles' survivability

6. Conclusions

Because the performance and survivability of geotextiles has a major effect on the economy of design, understanding and quantifying this is crucially important, and increasingly so as soil reinforcement technology because more and more prevalent. Therefore, the survivability of geotextiles should be verified by conducting tests under field conditions, especially for major projects. In the study reported in this paper, to assess installation damage at full-scale, a field test was employed to simulate unpaved road construction. Together with laboratory tests, this quantified the retained tensile strength of some geotextiles. Various parameters were investigated (four specially poor-graded fill materials, two kinds of subgrades with different CBR, three nonwoven needle-punched geotextiles with Classes 1, 2 and 3 (according to AASHTO M288-08) and two different relative densities for backfill materials). The results of the study, as applied to geotextile installations, can be summarized as follows:

• Neither fraying, fiber separation nor holes were observed. However, in all specimens, fine-grained particles were found to have entered into the texture of the geotextiles. Also, backfills with a median grain size of 12 and 16 mm, squeezed into the geotextiles' texture, especially in Class 2 and 3 types.

• The proposed models for predicting the ratio of retained tensile strength (S_r) and installation damage reduction factor (RF_{ID}) are highly representative of the measured results, even though their predictive ability is limited.

• The retained tensile strength of the geotextiles was significantly reduced as the median grain size (D_{50}) of the backfill increased.

• Tensile strengths of the geotextile decreased following placement of compacted fill to a high relative density. The greater compaction stress passed down to the geotextile, resulted in a greater reduction in the retained tensile strength.

• Selection of geotextiles with higher as-received grab tensile strength (increasing the geotextiles Class from 3 to 1) results in reduced installation damage.

• The subgrades' CBR is implicated in the amount of installation damage of geotextiles, probably due to its direct effect on the amount of extension in the geotextile layer caused by the imposed stress.

• The Dimensionless parameter of T_0 / (σD_{50}^2) implies that the change of geotextile damage will be more sensitive to change in median grain size of the backfill, with a power of two, as compared to changes in transferred stress, with a power of one.

This study investigated tensile strength reduction factors of nonwoven geotextiles for reinforcement and stabilization applications on low shear strength subgrades. Since, the obtained results are unlikely to be applicable to woven geotextiles, investigations on that material are highly recommended.

References

AASHTO M288-08 (2008), *Standard Specification for Geotextile Specification for Highway Applications*, American Association of State Highway and Transportation Officials, Virginia, U.S.A.

Allen, T.M. and Bathurst, R.J. (1994), "Characterization of geosynthetic load-strain behavior after installation damage", *Geosynth. Int.*, **1**(2), 181-199.

ASTM D 1556-08 (2008), *Standard Test Method for Density and Unit Weight of Soil in Place by Sand-Cone Method*, American Society for Testing and Materials, West Conshohocken, Pennsylvania, U.S.A.

ASTM D 5261-10 (2010), *Standard Test Method for Measuring Mass per Unit Area of Geotextiles, American Society for Testing and Materials*, West Conshohocken, Pennsylvania, U.S.A.

ASTM D 5821-13 (2013), *Standard Test Method for Determining the Percentage of Fractured Particles in Coarse Aggregate*, American Society for Testing and Materials, West Conshohocken, Pennsylvania, U.S.A.

ASTM D 6241-14 (2014), *Standard Test Method for Static Puncture Strength of Geotextiles and Geotextile-Related Products Using a 50-mm Probe*, American Society for Testing and Materials, West Conshohocken, Pennsylvania, U.S.A.

ASTM D4533-15 (2015), Standard Test Method for Trapezoidal Tearing strength of Geotextiles, 15American Society for Testing and Materials, West Conshohocken, Pennsylvania, U.S.A.

ASTM D4632-15 (2015), *Standard Test Method for Grab Breaking Load and Elongation of Geotextiles*, American Society for Testing and Materials, West Conshohocken, Pennsylvania, U.S.A.

ASTM D5818 (2000), *Obtaining Samples of Geosynthetics from a Test Section for Assessment of Installation Damage, American Society for Testing and Materials*, West Conshohocken, Pennsylvania, U.S.A.

Bathurst, R.J., Huang, B. and Allen, T.M. (2011), Analysis of installation damage tests for LRFD calibration of reinforced soil structures, *Geotext. Geomembr.*, **29**(3), 323-334.

Berg, R.R, Christopher, B.R. and Samtani, N.C. (2009), *Design of Mechanically Stabilized Earth Walls and Reinforced Soil Slopes*, FHWA NHI-10-024, Federal Highway Administration, Washington, U.S.A.

Carlos, D.M., Pinho-Lopes, M., Carneiro, J.R. and Lopes, M.L. (2015), "Effect of soil grain size distribution on the mechanical damage of nonwoven geotextiles under repeated loading", *Int. J. Geosynth. Ground Eng.*, **1**(1), 1-9.

Costa, C.M.L., Zornberg, J.G., Boeno, B.D.C. and Costa, Y.D.J. (2016), "Centrifuge evaluation of the time-dependent behavior of geotextile-reinforced soil walls", *Geotext. Geomembr.*, **44**(2), 188-200.

Deb, K. and Konai, S. (2014), "Bearing capacity of geotextile-reinforced sand with varying fine fraction", *Geomech. Eng.*, **6**(1), 33-45.

Elias, V. (2001), *Corrosion/Degradation of Soil Reinforcements for Mechanically Stabilized Earth Walls and Reinforced Soil Slopes*, FHWA-NHI-00-044, Federal Highway Administration, Washington, U.S.A.

Elvidge, C.B. and Raymond, G.P. (1999), "Laboratory survivability of nonwoven geotextiles on open-graded crushed aggregate", *Geosynth*. *Int*., **6**(2), 93-117.

FHWA-HI-95-038 (1998), *Geosynthetic Design and Construction Guidelines*, Federal Highway Administration, Washington, U.S.A.

Greenwood, J.H. and Brady, K.C. (1992), "Geotextiles in aggressive soils", *Construct*. *Build*. *Mater*., **6**(1), 15-18.

Hosseinpour, I., Almeida, M.S.S. and Riccio, M. (2015), "Full-scale load test and finite-element analysis of soft ground improved by geotextile-encased granular columns", *Geosynth*. *Int*., **22**(6), 428-438.

Hufenus, R., Rüegger, R., Flum, D. and Sterba, I.J. (2005), "Strength reduction factors due to installation damage of reinforcing geosynthetics", *Geotext*. *Geomembranes*, **23**(5), 401-424.

Kim, H.J., Won, M.S., Lee, J.B., Joo, J.H. and Jamin, J.C. (2015), "Comparative study on the behavior of soil fills on rigid acrylic and flexible geotextile containers", *Geomech*. *Eng*., **9**(2), 243-259.

Koerner, G.R. and Koerner, R.M. (1990), "The installation survivability of geotextiles and geogrids", *Proceedings of the 4th International Conference on Geotextiles, Geomembranes and Related Products*, The Hague, The Netherlands May-June.

Mendes, M.J.A., Palmeira, E.M. and Matheus, E. (2007), "Some factors affecting the in-soil load-strain behaviour of virgin and damaged nonwoven geotextiles", *Geosynth*. *Int*., **14**(1), 39-50.

Naeini, S.A. and Gholampoor, N. (2014), "Cyclic behaviour of dry silty sand reinforced with a geotextile", *Geotext*. *Geomembranes*, **42**(6), 611-619.

Nikbakht, M. and Diederich, R. (2008), "The energy potential and its integration in the national European specification", *Found*. *Civ*. *Environ*. *Eng*., (11), 41-53.

Pinho-Lopes, M. and Lopes, M.L. (2013), "Tensile properties of geosynthetics after installation damage", *Environ*. *Geotech*., **1**(3), 161-178.

Portelinha, F.H.M, Bueno, B.S. and Zornberg, J.G. (2013), "Performance of nonwoven geotextile-reinforced walls under wetting conditions: Laboratory and field investigations", *Geosynth*. *Int*., **20**(2), 90-104.

Portelinha, F.H.M., Zornberg, J.G. and Pimentel, V. (2014), "Field performance of retaining walls reinforced with woven and nonwoven geotextiles", *Geosynth*. *Int*., **21**(4), 270-284.

Richardson, G.N. (1998), "Field evaluation of geosynthetic survivability in aggregate road base", Geotechnical Fabrics Report, **16**, 34-38.

Rosete, A., Lopes, P.M., Pinho-Lopes, M. and Lopes, M.L. (2013), "Tensile and hydraulic properties of geosynthetics after mechanical damage and abration laboratory tests", *Geosynth*. *Int*., **20** (5), 358-374.

Tandel, K.Y., Solanki, C.H. and Desai A.K. (2014), "Field behaviour geotextile reinforced sand column", *Geomech*. *Eng*., **6**(2), 195-211.

Tavakoli Mehrjardi, Gh. and Amjadi Sardehaei, E., (2017). "Design graphs to estimate reduction factor of nonwoven geotextiles due to installation process", *Eur*. *J*. *Environ*. *Civ*. *Eng*., 1-14.

Tavakoli Mehrjardi, Gh., Ghanbari, A. and Mehdizadeh, H. (2016), "Experimental study on the behaviour of geogrid-reinforced slopes with respect to aggregate size", *Geotext*. *Geomembranes*, **44**(6), 862-871.

Tavakoli Mehrjardi, Gh., Moghaddas Tafreshi, S.N. and Dawson, A.R. (2013), "Pipe response in a geocell reinforced trench and compaction considerations", *Geosynth*. *Int*., **20**(2), 105-118.

Vieira, C.S. and Pereira, P.M. (2015), "Damage induced by recycled construction and demolition wastes on the short-term tensile behaviour of two geosynthetics", *Transport*. *Geotech*., **4**(September), 64-75.

Vieira, C.S., Lopes , M.D.L. and Caldeira, L. (2015), "Sand-Nonwoven geotextile interfaces shear strength by direct shear and simple shear tests", *Geomech*. *Eng*., **9**(5), 601-618.

Wang, L., Zhang, G. and Zhang, J.M. (2011), "Centrifuge model tests of geotextile-reinforced soil embankments during an earthquake", *Geotext*. *Geomembr*., **29**(3), 222-232.

Watn, A., Eiksund, G. and Knutson, A. (1998), "Deformation and damage of nonwoven geotextiles in road construction", *Proceedings of the 6th International Conference on Geosynthetics*, Atlanta, Georgia, U.S.A., March.

Watts, G.R.A. and Brady, K.C. (1994), "Geosynthetics-installation damage and the measurement of tensile strength", *Proceedings of the 5th International Conference on Geotextiles, Geomembranes and Related Products*, Singapore, September.

WSDOT T925 (2005), *Standard Practice for Determination of Long-Term Strength for Geosynthetic Reinforcement*, Washington State Department of Transportation, Olympia, Washington, U.S.A.

CC

Nomenclature

Meaning	Units	Symbol
Coefficient of uniformity	-	C_u
Coefficient of curvature	-	C_c
Subgrade CBR	(%)	CBR
Coarse-grained subgrade	-	CS
Backfill's relative density	(%)	D_r
Effective grain size	(mm)	D_{10}
Grain size of 30% passing percentage	(mm)	D_{30}
Median grain size	(mm)	D_{50}
Grain size of 60% passing percentage	(mm)	D_{60}
Fine-grained subgrade	-	FS
Specific gravity of soil	-	G_s
Coefficient of Regression	-	R^2
Installation damage reduction factor of geotextile	-	RF_{ID}
Ratio of retained strength of geotextile	-	S_r
Transferred stress at the level of geotextile	(Pa)	σ

As-received grab tensile strength of the geotextiles	(N)	T_0
Retained grab tensile strength of the geotextiles	(N)	T_{ID}
Characteristic parameter	-	$T_0/(\sigma D_{50}^2)$